Realization of an Optimally Distinguishable Multiphoton Quantum Superposition

Francesco De Martini, Fabio Sciarrino, and Veronica Secondi

Dipartimento di Fisica and Istituto Nazionale di Fisica per la Materia, Universitá "La Sapienza," Roma 00185, Italy

(Received 15 June 2005; published 5 December 2005)

We report the realization of an entangled quantum superposition of $M \sim 12$ photons by multiple universal cloning of a single-photon qubit via the high gain, quantum-injected optical parametric amplification. The system has been found extremely resilient to decoherence. By quantum tomography, the nonseparability and the quantum superposition are demonstrated for the mesoscopic output state of the dynamic "closed system."

DOI: 10.1103/PhysRevLett.95.240401 PACS numbers: 03.65.Ta, 03.67.Mn, 42.50.Ar, 42.50.Xa

Since the golden years of quantum mechanics, the interference of classically distinguishable quantum states, first epitomized by the famous "*Schrödinger cat*" apologue [1], has been the object of extensive theoretical studies and recognized as a major conceptual paradigm of physics [2]. In modern times, the sciences of quantum information and quantum computation deal precisely with collective processes involving a multiplicity of interfering states, generally mutually entangled and rapidly dephased by decoherence [3]. In many respects, the implementation of this intriguing classical-quantum condition represents today an unsolved problem, in spite of recent successful studies carried out mostly with atoms and ions [4,5]. The present work reports on a virtually decoherence-free scheme based on the quantum-injected optical parametric amplification (QI-OPA) of a single photon in a quantum superposition state of polarization (π), i.e., a π-encoded qubit [6,7]. Conceptually, the method consists of transferring the well accessible condition of quantum superposition of a 1-photon qubit, $N = 1$, to a *mesoscopic,* i.e., multiphoton amplified state $M \gg 1$, here referred to as a "mesoscopic qubit" (M qubit). This can be done by injecting in the QI-OPA the 1-photon qubit $\alpha|H\rangle + \beta|V\rangle$, here expressed in terms of two orthogonal π states, e.g., horizontal and vertical linear π: $|H\rangle$, $|V\rangle$. In virtue of the general information preserving property of the OPA, the generated state is found to be entangled and to keep the same superposition character and the interfering properties of the injected qubit [6]. Since the present scheme realizes the deterministic $1 \rightarrow M$ universal optimal quantum cloning machine (UOQCM), i.e., is able to copy optimally any unknown input qubit into $M \gg 1$ copies with the same "fidelity," the output state will be necessarily affected by squeezed-vacuum noise arising from the input vacuum field.

Let us refer to the apparatus: Fig. 1. The active element was a nonlinear (NL) crystal slab (BBO: β-barium borate), 1.5 mm thick cut for type II phase matching, able to generate by spontaneous parametric down-conversion (SPDC) $\vec{\pi}$-entangled photon pairs. The OPA *intrinsic phase* was set as to generate by SPDC singlet states on the output modes, a condition assuring the universality of the present cloning transformation [6,8–10]. The excitation source was a Ti:Sa mode-locked laser further amplified by a Ti-Sa regenerative device (A) operating with pulse duration 180 fs at a repetition rate 250 kHz, average power 1 W. By (A), the OPA gain was enhanced by a factor $\simeq 17$ with respect to earlier experiments [8–10]. The output beam, frequency doubled by second harmonic generation (SHG), provided the excitation beam with UV wavelength (WL) $\lambda_P = 397.5$ nm and energy per pulse $E_{\mathrm{UV}}^{\mathrm{HG}} = 1\ \mu$J. The "seed" photon pairs were emitted, with a coherence time ≈ 500 fs, by an OPA process acting towards the right-hand side of Fig. 1 with equal WL's $\lambda = 795$ nm over two spatial modes $-\mathbf{k}_1$ and $-\mathbf{k}_2$ owing to a SPDC process excited by the UV beam associated with mode $-\mathbf{k}_p$ with WL λ_p. The UV beam was back-reflected over the mode $\mathbf{k}_p$ onto the NL crystal by a spherical mirror $\mathbf{M}_p$, with μ-metrically adjustable position $\mathbf{Z}$, thus exciting the main OPA "cloning" process towards the left-hand

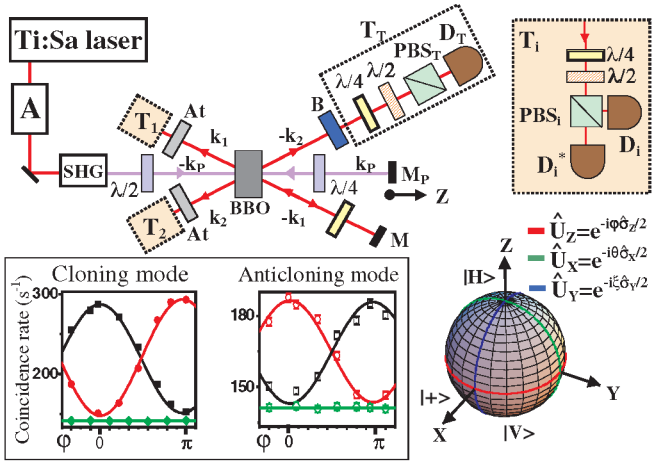

FIG. 1 (color online). Layout of the quantum-injected OPA apparatus; T_i ($i = 1, 2$) QST setup; Bloch sphere representation of the input qubit. Inset: Mesoscopic interference fringe patterns measured over the modes $\mathbf{k}_i$ vs the phase φ for the $\hat{U}_Z$ map. The continuous lines express the best fit results.

side of Fig. 1. By the combined effect of two adjustable optical UV wave plates (WP's) ($\lambda/2 + \lambda/4$) acting on the projections of the linear polarization π_p^{UV} on the optical axis of the BBO crystal for the $-\mathbf{k}_p$ and $\mathbf{k}_p$ excitation processes, the seed SPDC excitation was always kept at a low level while driving the main OPA to a high gain (HG) regime. Precisely, by smartly unbalancing the orientation of the axes of the UV WP's, the SPDC emission probability towards the right-hand side of Fig. 1 of 2 simultaneous photon pairs was always kept below the one of single pair emission by a factor $\sim 3 \times 10^{-2}$. One of the photons of the seed SPDC pair, back-reflected by a fixed mirror **M**, was *reinjected* after a $\vec{\pi}$ flipping by a $\lambda/4$ WP onto the NL crystal over the input mode $\mathbf{k}_1$, while the other photon emitted over mode $(-\mathbf{k}_2)$ excited the detector D_T, the trigger of the overall conditional experiment. The entangled state of the seed pair after M reflection and $\vec{\pi}$ flipping was $|\Phi^-\rangle_{-k2,k1} = 2^{-1/2}(|H\rangle_{-k2}|H\rangle_{k1} - |V\rangle_{-k2}|V\rangle_{k1})$. By virtue of the nonlocal correlation acting on the seed modes $-\mathbf{k}_1$ and $-\mathbf{k}_2$, the input qubit was prepared on mode $\mathbf{k}_1$ in the *pure* state $|\Psi\rangle_{\mathrm{in}} = \alpha|H\rangle_{k1} + \beta|V\rangle_{k1}$, $|\alpha|^2 + |\beta|^2 = 1$ by the combined action of the $\lambda/2$ WP, of the $\lambda/4$ WP (WP_T), of the adjustable Babinet compensator (B), and of a polarizing beam splitter (PBS_T) acting on mode $-\mathbf{k}_2$. This device allowed all orthogonal transformations $\hat{U}_X$, $\hat{U}_Y$, $\hat{U}_Z$ on the Bloch sphere of the input qubit: Fig. 1, inset. The quantum state tomography (QST) devices T_T, T_i ($i = 1, 2$) were equipped with equal single-photon fiber coupled SPCM-AQR14-FC detectors (D) with quantum efficiencies $\eta_D \simeq 60\%$, and equal interference filters with bandwidth $\Delta\lambda = 4.5$ nm were placed in front of each D: Fig. 1, inset.

Let us rewrite $|\Psi\rangle_{\mathrm{in}}$ by expressing the interfering states as Fock product states: $|H\rangle_{k1} = |1\rangle_{1H}|0\rangle_{1V}|0\rangle_{2H}|0\rangle_{2V} \equiv |1, 0, 0, 0\rangle$; $|V\rangle_{k1} = |0, 1, 0, 0\rangle$, accounting for 1 photon on the input $\mathbf{k}_1$ with different orthogonal $\vec{\pi}$'s and vacuum on the input $\mathbf{k}_2$. It evolves into the output state $|\Psi\rangle = \hat{U}|\Psi\rangle_{\mathrm{in}}$ according to the main OPA unitary $\hat{U}$ process [10]. The output state $\tilde{\rho} = (|\Psi\rangle\langle\Psi|)$ over the modes $\mathbf{k}_1, \mathbf{k}_2$ of the QI-OPA apparatus is found to be expressed by the M qubit:

$$|\Psi\rangle = \alpha|\Psi\rangle^H + \beta|\Psi\rangle^V, \tag{1}$$

where $|\Psi\rangle^H = \sum_{i,j=0}^{\infty} \gamma_{ij}\sqrt{i+1}|i+1, j, j, i\rangle$, $\gamma_{ij} \equiv (-\Gamma)^i \times \Gamma^j \cosh^{-3} g$, $\Gamma \equiv \tanh g$, $|\Psi\rangle^V = \sum_{i,j=0}^{\infty} \gamma_{ij}\sqrt{j+1}|i, j+1, j, i\rangle$, the parameter g expressing the NL "gain" [8]. These interfering entangled, multiparticle states are *orthonormal*, i.e., $|^i\langle\Psi \mid \Psi\rangle^j|^2 = \delta_{ij}$ $\{i, j = H, V\}$, and pure, i.e., fully represented by the operators $\rho^H = (|\Psi\rangle\langle\Psi|)^H$, $\rho^V = (|\Psi\rangle\langle\Psi|)^V$. Hence, the pure state $|\Psi\rangle$ is a quantum superposition of two multiphoton pure states and bears the same superposition properties of the injected qubit. In addition, it is highly significant in the present context to consider the output pure state $|\Sigma\rangle$ of the overall apparatus, including the "trigger" that enters in the dynamics through the Bell state $|\Phi^-\rangle_{-k2,k1}$. This state [11] expresses the entanglement of all output modes $\mathbf{k}_1$, $\mathbf{k}_2$, and $-\mathbf{k}_2$, thus eliciting a peculiar cause-effect dynamics within the overall "closed" system:

$$|\Sigma\rangle \equiv 2^{-1/2}(|H\rangle_{-k2}|\Psi\rangle^H - |V\rangle_{-k2}|\Psi\rangle^V). \tag{2}$$

The experimental investigation of the multiphoton superposition and entanglement implied by Eqs. (1) and (2) was carried out by means of the T_i, T_T devices according to a "loss method" first applied to SPDC in Ref. [12]. The beams associated with the output modes $\mathbf{k}_i$ ($i = 1, 2$) were highly attenuated to the single-photon level by the two low transmittivity beam splitters (At) in Fig. 1. Since the bipartite entanglement affecting the multiphoton $\mathbf{k}_i$ ($i = 1, 2$) also implies a correlation of the single photons detected on either mode and since it is impossible to create or enhance entanglement by *local* operations, e.g., by the loss mechanism acting over each mode, the entanglement detected at the *single-photon* level over $\mathbf{k}_i$ ($i = 1, 2$) necessarily implies the same property to affect the same modes in the multiphoton condition [12]. In agreement with the loss method, we investigated by two different QST experiments the *reduced* density matrices ρ and ρ', i.e., the single-photon counterparts of the multiphoton states $\tilde{\rho} = |\Psi\rangle\langle\Psi|$, $\tilde{\rho}' = |\Sigma\rangle\langle\Sigma|$. The experimental results, reported in Figs. 2 and 3, respectively, are compared with the corresponding theoretical ρ^{th} and ρ'^{th}, which have been calculated by a numerical algorithm performing the multiple tracing of $\tilde{\rho}$, $\tilde{\rho}'$ over all photons discarded by the At devices on the modes $\mathbf{k}_i$ ($i = 1, 2$). Theoretical details on this most useful algorithm and on the overall experiment will be given in a forthcoming comprehensive paper [13]. In order to carry out the calculations properly, the maximum value of the gain g_{exp} and of the overall quantum efficiencies η_i of the detection apparatuses acting on $\mathbf{k}_i$ ($i = 1, 2$) were measured. It was found that $g_{\mathrm{exp}} = 1.19 \pm 0.05$ and $\eta_1 = (4.9 \pm 0.2)\%$; $\eta_2 = (4.2 \pm 0.2)\%$.

Let us now address the main goal of the present work, i.e., the detection and characterization of the output states. The interference character of the output field implied by the quantum superposition character of the input qubit $|\Psi\rangle_{\mathrm{in}} = 2^{-1/2}(|H\rangle + e^{i\varphi}|V\rangle)$ was detected simultaneously in the basis $|\pm\rangle \equiv 2^{-1/2}(|H\rangle \pm |V\rangle)$ over the output cloning mode $\mathbf{k}_1$ and "anticloning" $\mathbf{k}_2$ by the $2 - D$ coincidences $[D_i, D_T]$ (squares in Fig. 1 inset) and $[D_i^*, D_T]$ (circles) ($i = 1, 2$). Precisely, the interference fringe patterns correspond to $\hat{U}_Z$ transformations on the input Bloch sphere, i.e., implying changes of the phase φ. The fringe "visibility" ($\mathcal{V}$) measured over $\mathbf{k}_1$ was found to be gain-dependent $\mathcal{V}_1^{\mathrm{th}}(g) = (1 + 2\Gamma^2)^{-1}$ as predicted by theory [6]. The experimental value $\mathcal{V}_1 = (32 \pm 1)\%$ should be compared with the theoretical one: $\mathcal{V}_1^{\mathrm{th}}(g_{\mathrm{exp}}) = 42\%$. By setting $g = \Gamma = 0$, the effective visibility of the input qubit was measured: $\mathcal{V}_{\mathrm{in}} \approx 87\%$. The $\mathcal{V}$ value for the $\mathbf{k}_2$ mode $\mathcal{V}_2 = (13 \pm 1)\%$ should be compared with the theoretical: $\mathcal{V}_2^{\mathrm{th}} = 33\%$ [6]. All these discrepancies are mainly attributed to unavoidable walk-off effects in the NL slab spoiling the critical superposition of the injection and

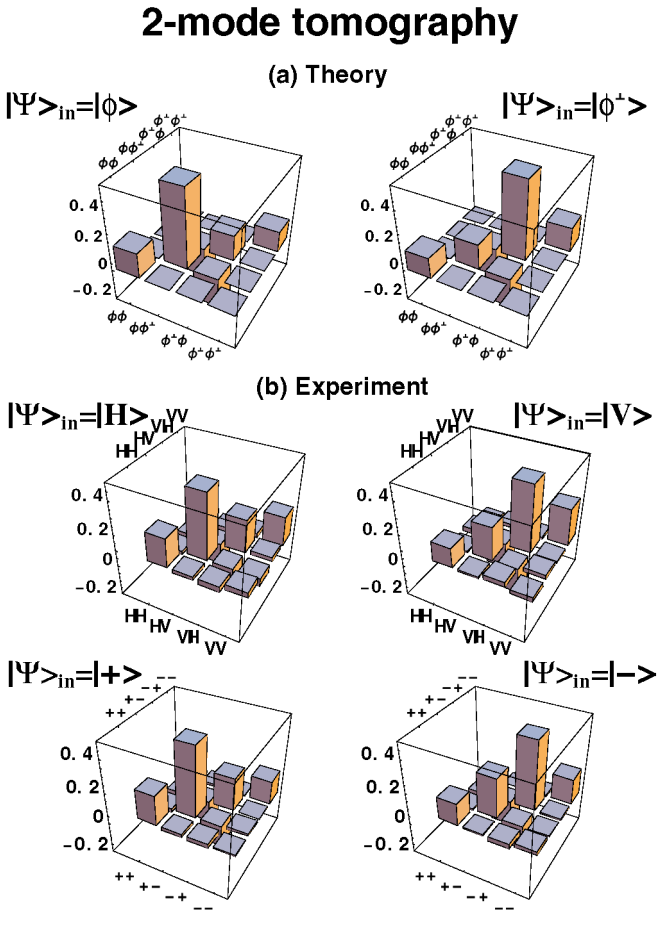

FIG. 2 (color online). QST plots of the reduced two-photon output state over the output modes $\mathbf{k}_i$ $(i = 1, 2)$ conditioned by the injection of a generic polarization qubit $|\Psi\rangle_{\text{in}} = |\phi\rangle$ on the mode $\mathbf{k}_1$. (a) Theoretical simulation. (b) Experimental results. The imaginary components are negligible on the adopted scale.

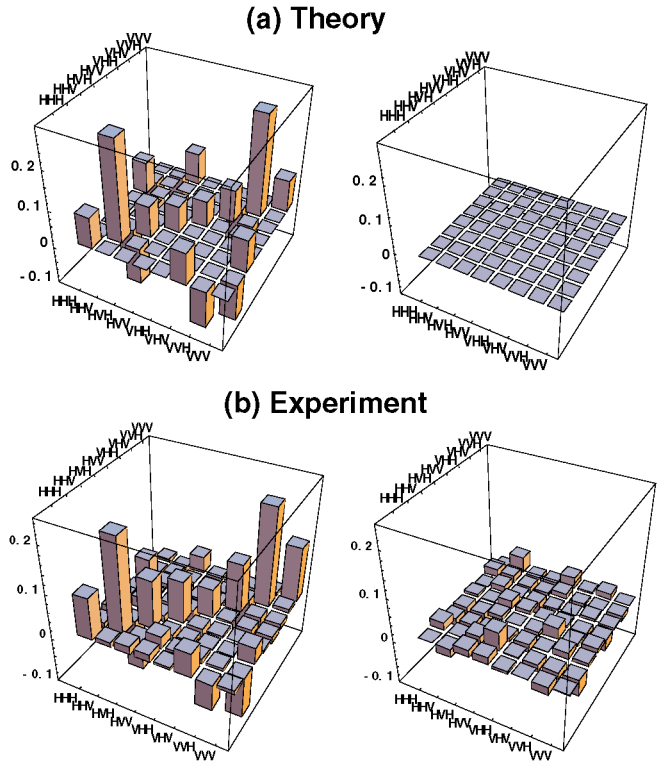

FIG. 3 (color online). QST plots of the reduced overall output state over the modes $-\mathbf{k}_2$, $\mathbf{k}_i$ $(i = 1, 2)$ under the condition of lossy channels for the multiphoton modes $\mathbf{k}_i$. The experimental density matrix ρ'^{exp} has been reconstructed by measuring 64 - three-qubit observables and by applying a linear inversion reconstruction. Each QST run lasted 60 s and yielded a maximum 1866 threefold counts for the $|HHV\rangle$ projection. The uncertainties of the data were evaluated by a numerical simulation assuming Poissonian fluctuations. The imaginary plots are reported at the right-hand side of the figure.

pump pulses in the birefringent active region. The overall average number of the stimulated emission photons per pulse over $\mathbf{k}_i$ $(i = 1, 2)$ was found, in the quantum-injected HG regime, $M = (11.1 \pm 1.3)$, a result consistent with the value of g measured by an entirely different experiment. Precisely, the average number of photons generated on the cloning mode was $M_C = 6.1 \pm 0.9$, and the average fidelity, obtained by the corresponding $\mathcal{V}$ value on the same mode, was $F_C = (1 + V_1)/2 = 66.2 \pm 0.5$. Note that, for $M \to \infty$, viz. $g \to \infty$ and $\Gamma \to 1$, the "fringe visibility" and the fidelity attain the asymptotic values $\mathcal{V}_1^{\text{th}} = \mathcal{V}_2^{\text{th}} = 33\%$ and $F_C = F_{AC} = (2/3)$. In the present experiment, because of the unavailability on the market of reliable photon number-resolving detectors, the measurement of M and M_C was transformed into a detection rate measurement owing to $\eta_1 \sim \eta_2 \ll 1$.

A most insightful state analysis was provided by a full QST study of the output ρ and ρ', as said. Figure 2 shows the QST analysis of the reduced output state ρ determined by the set of input $|\Psi\rangle_{\text{in}}$: $\{|H\rangle, |V\rangle, |\pm\rangle\}$. The experimental data ρ^{exp} shown by Fig. 2(b) were obtained by a 3D coincidence method $[D_T, D_1, D_2]$ for different settings of the QST setups T_i. The good agreement between theory and experiment is expressed by the measured average Uhlmann fidelity: $\mathcal{F}(\rho^{\text{exp}}, \rho^{\text{th}}) \equiv [\text{Tr}(\sqrt{\rho^{\text{exp}}}\rho^{\text{th}}\sqrt{\rho^{\text{exp}}})^{1/2}]^2 = (96.6 \pm 1.2)\%$. In Figs. 2(a) and 2(b), the structure of the 4×4 matrices ρ shows the relevant quantum features of the output state. For instance, the highest peak on the diagonals expressing the quantum superposition of the input state shifts from the position $|\phi\phi^{\perp}\rangle\langle\phi\phi^{\perp}|$ to $|\phi^{\perp}\phi\rangle\langle\phi^{\perp}\phi|$ in correspondence with the OPA excitation by any set of generic orthogonal injection states $\{|\phi\rangle, |\phi^{\perp}\rangle\}$, i.e., represented by the maxima and minima of the fringe patterns of Fig. 1, inset. The experimental patterns of Fig. 2(b) obtained by injection of different basis sets $\{|H\rangle, |V\rangle\}$ and $\{|+\rangle, |-\rangle\}$ indeed confirm the "universality" of this process, i.e., reproducing identically for any couple of orthogonal input states. As expected, the interference effect and the fringe pattern of Fig. 1, inset, was found to dis-

appear in the absence of the injection qubit (rhombohedrons in Fig. 1, inset) [13]. The application to all ρ matrices shown in Fig. 2(b) of the Peres-Horodecki positive partial transpose (PPT) criterion ensures the nonseparability of the reduced state ρ and then, necessarily, of the corresponding "true" multiphoton output state $\tilde{\rho}$, as said [12,14]. Indeed, the minimal eigenvalue of the partial transpose of the "theoretical" matrices ρ^{th} of Fig. 2(a) was found to be *negative*, $\lambda_{\mathrm{min}} = -0.046$, a result reproduced by all ρ^{exp} reported in Fig. 2(b). For instance, for ρ^{exp} determined by $|\Psi\rangle_{\mathrm{in}} = |-\rangle$, it was found that $\lambda = -0.014 \pm 0.0025$ for $g_{\mathrm{exp}} \sim 1.19$. Let us turn our attention to the state ρ' correlating all output modes: Fig. 3(b). The QST reconstruction was achieved by the devices T_T, T_i, again with a large fidelity: $\mathcal{F}(\rho'^{\mathrm{exp}}, \rho'^{\mathrm{th}}) = (85.0 \pm 1.1)\%$. The quantum superposition of the output state is expressed here by the off-diagonal elements of both matrices ρ'^{th}, ρ'^{exp}. Once again, the nonseparability of ρ' for the bipartite system $-\mathbf{k}_2$ and $\{\mathbf{k}_1, \mathbf{k}_2\}$ was proved by the PPT method, a sufficient criterion for three-qubit mixed states. Again, the minimal eigenvalue of the transpose of both matrices ρ' in Fig. 3 was found to be negative: $\lambda'_{\mathrm{min}} = -0.024$ and $\lambda'_{\mathrm{exp}} = -0.021 \pm 0.004$. This proves the nonseparability of the true tripartite pure state $\tilde{\rho}'$, Eq. (2) correlating the trigger and the multiphoton $\mathbf{k}_i$ modes within a "closed box."

A striking property of the present system is its extreme resilience to decoherence, as shown by the interference patterns of Fig. 1. Since in our system decoherence is determined only by stray reflection losses on the single output surface of the NL crystal, a photon number $M > 10^3$ could be easily excited in quantum superposition. More precisely, we have found that the visibilities $\mathcal{V}_i^{\mathrm{th}}$ drop to half of their maximum values upon stray photon losses larger than 92%, while in other systems, e.g., involving atoms and photons in a superconducting QED cavity, the loss of *only one* photon kills the interference [3,4]. Consequently, in our system the mesoscopic superposition is *directly accessible* at the output of the apparatus at normal, i.e., room, temperature (T). This lucky result is partially attributed to the minimum Hilbert-Schmidt (d) "distance" on the phase space of the interfering states realized here: $d(\rho^H; \rho^V) = \mathrm{Tr}[(\rho^H - \rho^V)^2] = 2$ [15]. The limited, i.e., *optimal,* distinguishability of the mesoscopic states is attributed to the present single particle, *cloningwise,* π-measurement method. However, the exact distinguishability implied by the orthogonality of $|\Psi\rangle^H$ and $|\Psi\rangle^V$ could be attained by any measurement protocol identifying in a *cumulative* fashion all M output particles [16].

In summary, we have demonstrated the interference of mesoscopic, orthonormal, pure states in agreement with the quantum theoretical results, Eqs. (1) and (2). The adoption of "periodic-poled" nonlinearities is expected to further increase g by a factor $\gtrsim 2$ and the value of M at least by an order of magnitude. On a conceptual side, our system is expected to open a new trend of studies on the persistence of the validity of crucial laws of quantum mechanics for entangled mixed-state systems of increasing complexity [4] and on the violation of Bell inequalities in the multiparticle regime [17]. In addition, it suggests a plausible signal-amplification model for the establishment of collective coherence effects in complex biological systems at normal T, e.g., within the search of any noncomputable physical process in the self-conscious brain [18].

This work was supported by the FET EU (IST-2000-29681: ATESIT). We thank M. Caminati and R. Perris for the experimental support.

Note added in proof.—Owing to experimental improvements and a better tuning of the lasers, the following parameters have been attained: $g \approx 2.2$, $M \approx 50$. Demonstration of entanglement for $M > 12$ is in progress.

[1] E. Schrödinger, Naturwissenschaften **23**, 807 (1935).

[2] A. Caldeira *et al.*, Physica (Amsterdam) **121A**, 587 (1983); A. Leggett *et al.*, Phys. Rev. Lett. **54**, 857 (1985).

[3] W. Zurek, Phys. Today **44**, No. 10, 36 (1991).

[4] M. Brune *et al.*, Phys. Rev. Lett. **77**, 4887 (1996); A. Auffeves *et al.*, Phys. Rev. Lett. **91**, 230405 (2003); P. Maioli *et al.*, Phys. Rev. Lett. **94**, 113601 (2005).

[5] C. Monroe *et al.*, Science **272**, 1131 (1996); D. Leibfried *et al.*, Science **304**, 1476 (2004); C. F. Roos *et al.*, Science **304**, 1478 (2004).

[6] F. De Martini, Phys. Rev. Lett. **81**, 2842 (1998). Larger values up to $\mathcal{V}_2^{\mathrm{th}} > 50\%$ are offered by less universal schemes, e.g., by mode-degenerate *phase-covariant* cloning: F. De Martini, Phys. Lett. A **250**, 15 (1998).

[7] F. De Martini *et al.*, Phys. Rev. Lett. **87**, 150401 (2001).

[8] F. De Martini *et al.*, Nature (London) **419**, 815 (2002).

[9] A. Lamas-Linares *et al.*, Science **296**, 712 (2002).

[10] D. Pelliccia *et al.*, Phys. Rev. A **68**, 042306 (2003); F. De Martini *et al.*, Phys. Rev. Lett. **92**, 067901 (2004).

[11] W. P. Schleich, *Quantum Optics in Phase Space* (Wiley, New York, 2001), Chaps. 11 and 16.

[12] H. S. Eisenberg *et al.*, Phys. Rev. Lett. **93**, 193901 (2004); G. A. Durkin *et al.*, Phys. Rev. A **70**, 062305 (2004).

[13] M. Caminati, R. Perris, F. Sciarrino, V. Secondi, and F. De Martini, quant-phys/0510153.

[14] A. Peres, Phys. Rev. Lett. **77**, 1413 (1996).

[15] M. Nielsen *et al.*, *Quantum Computation and Information* (Cambridge University, Cambridge, England, 2000), Chap. 9.

[16] A cumulative procedure could be as follows. Assume that the number of emitted photons is determined exactly by adopting ideal detectors $D_{i\pi}$ with $\eta_D = 1$ coupled to the output modes $\mathbf{k}_i$ with polarizations π ($i = 1, 2$; $\pi = h, v$). According to Eq. (1), $|\Psi\rangle^H$ is identified *exactly* if the total photon number detected by the couple $\{D_{1h} + D_{2v}\}$ is *odd* and the one by $\{D_{1v} + D_{2h}\}$ is *even*. The opposite result identifies the state $|\Psi\rangle^V$ exactly.

[17] M. D. Reid *et al.*, Phys. Rev. A **66**, 033801 (2002).

[18] R. Penrose, *The Large, the Small and the Human Mind* (Cambridge University Press, Cambridge, England, 2000), Chap. 3.